Proceedings of CHT-17
ICHMT International Symposium on Advances in Computational Heat Transfer

May 28-June 1, 2017, Napoli, Italy

CHT-17-216

NUMERICAL SIMULATION OF FLUID BEHAVIORS UNDER INFLUENCING FACTORS OF CRYOGENIC CAPILLARY-FLOW UNDER MICROGRAVITY

Rong Ma[§], Wei Yao, Chao Wang, Xiaochen LU
China Academy of Space Technology, Beijing, China
[§]Correspondence author. Fax: +86 10 68747505 Email: rong.jessica@hotmail.com

ABSTRACT As the surface tension of cryogenic fluids in deep low-temperature space is much smaller, the capillary driven by surface tension is weakened under microgravity, which is influenced by many factors, including the working fluid properties, the wettability of capillary surface, and the geometrical properties of tube (cross-sectional shape, equivalent diameter, wetted perimeter, etc.). So it is necessary to study the flow behaviors of low temperature working fluid driven by surface tension under microgravity. In the paper, fluid behaviors under influencing factors (including tube sizes, low-temperature working fluid properties, initial liquid volumes, etc.) of cryogenic capillary-flow under microgravity are studied numerically by developing a 2D numerical simulation of vertical capillary tube. In the process of direct numerical simulation, the interface between two phases is represented by a boundary and has no thickness which is described through the moving mesh interface method. To verify accuracy and rationality of this numerical method, the capillary height of interphase between water and air at room temperature in the gravity field is tested firstly, in which the relative results prove that the accuracy and rationality of this numerical method here. Then, the numerical simulation is carried out for four working cases, which is also analyzed in detail. The work in this paper can provide effective verification and analysis means for subsequent experiments and theoretical models.

INTRODUCTION

With the rapid development of human space exploration and space science, the capillary flow has drawn much more attention in recent years [e.g. Lucas 1918, Washburn 1921, Bell 1906], because of its importance for fluid dynamics, surface science and especially for fluid management in space including propellant and cryogenic fluid tanks, thermal control systems, coolant reservoirs and systems for collection, storage and provision of water [Dreyer 1998]. Capillary flows are spontaneous interfacial flows driven by surface tension, container geometry and surface wettability without the ubiquitous effects of gravity, which are fundamental to a myriad transport processes in both nature and industry and range from microscale flows ($\leq 1mm$) in porous media on earth to macroscale flows ($\leq 1m$) in large liquid fuel tanks aboard spacecraft. In the space microgravity environment, the surface tension highlights in the gas-liquid two-phase fluid flow and its phase change heat transfer process is prominent and dominant, which plays the leading role.

As the capillary-driven flow becomes remarkable only when the size of the capillary tube is small for terrestrial experiments, many researchers have begun to experimentally study the capillary-driven flow under microgravity because large sized capillary tubes can be used by removing the effect of gravity [e.g. Dreyer 1994, Weislogel 1998, Chen 2005, Concus 2000, Stange 2003, Wang 2009]. However, for

cryogenic fluids in deep low-temperature space, the surface tension is much smaller, and the capillary driven by surface tension is weakened under microgravity. So it is necessary to study the flow behaviors of low temperature working fluid driven by surface tension under microgravity. Under microgravity, flow behaviors of cryogenic fluids are rather complicated, because the dynamic process of the interface evolution is influenced by many factors, including the working fluid properties, the wettability of capillary surface, and the geometrical properties of tube (cross-sectional shape, equivalent diameter, wetted perimeter, etc.). So far, there is still a lack of systematic study on effects of these factors on the capillary flow behaviors and dynamics under microgravity.

As one of the most important means of modern scientific research, numerical simulation has been widely used in the research of multiphase flow because of its outstanding superiority. In view of the complexity and high cost of the test, a 2D numerical simulation of fluid behaviors under influencing factors (including tube sizes, low-temperature working fluid properties, initial liquid volumes, etc.) of cryogenic capillary-flow under microgravity is carried out in this paper, which can provide effective verification and analysis means for subsequent experiments and theoretical models.

NUMERICAL METHOD

The interface between two phases is represented by a boundary and has no thickness which is described through the moving mesh interface method.

Governing Equations With assumptions of immiscible, incompressible Newtonian fluids, the Navier-Stokes equations are expressed as below:

$$\nabla \cdot \mathbf{u} = 0 \tag{1}$$

$$\rho\left(\frac{\partial \mathbf{u}}{\partial t} + (\mathbf{u} - \mathbf{u_m}) \cdot \nabla \mathbf{u}\right) = -\nabla p + \rho \mathbf{g} + \nabla \cdot \left[\mu\left(\nabla \mathbf{u} + (\nabla \mathbf{u})^{\mathrm{T}}\right)\right] + \mathbf{F}_{\sigma} \tag{2}$$

where ρ is the fluid density, $\boldsymbol{u}$ is the velocity vector, μ is the fluid viscosity, p is the pressure, and $\boldsymbol{g}$ is the gravitational acceleration, $\boldsymbol{F}_{\sigma}$ denotes the surface tension force, $\boldsymbol{u}$m denotes the mesh velocity and arises from the definition of time derivatives in the coordinate system of the deformed mesh. Poisson's equation is solved for the mesh displacement.

Boundary Conditions In the absence of mass flow across the boundary the correct boundary condition on the fluid/fluid interface is

$$\mathbf{n} \cdot (\mathbf{T}_1 - \mathbf{T}_2) = \sigma(\nabla \cdot \mathbf{n})\mathbf{n} - \nabla \sigma \tag{3}$$

where the total stress tensor, T is defined for either fluid 1 or fluid 2 as

$$\mathbf{T}_{1,2} = -p_{1,2}\mathbf{I} + \eta_{1,2}(\nabla \mathbf{u}_{1,2} + (\nabla \mathbf{u}_{1,2})^{T}) \tag{4}$$

This boundary condition can be decomposed into a normal component

$$\mathbf{n} \cdot \mathbf{T}_1 \cdot \mathbf{n} - \mathbf{n} \cdot \mathbf{T}_2 \cdot \mathbf{n} = \sigma(\nabla \cdot \mathbf{n}) \tag{5}$$

and a tangential component

$$\mathbf{n} \cdot \mathbf{T}_1 \cdot \mathbf{t} - \mathbf{n} \cdot \mathbf{T}_2 \cdot \mathbf{t} = \nabla \sigma \cdot \mathbf{t} \tag{6}$$

The term on the right-hand side of Equation 5 is the force per unit area due to local curvature of the interface. The term on the right-hand side of Equation 6 is a tangential stress associated with gradients in the surface tension coefficient. Equation 6 reveals that whenever gradients in the surface tension coefficient exist, the flow must be nonstationary. This is because the pressure is continuous in the tangential direction so the gradient in the surface tension coefficient must be balanced by the tangential

component of the viscous stress. A mesh velocity equal to the fluid velocity is imposed on the interface:

$$\mathbf{u}_m = \mathbf{u} \tag{7}$$

Equation 1 and Equation 2 along with the equation for the mesh displacement describe the evolution of the fluid at the domain level. Equation 3 and Equation 7 are suitable boundary conditions for the problem. These equations and boundary conditions are solved in the moving mesh interface method.

COMPUTATION CONDITIONS

Geometry Model, Boundary Conditions and Initial Conditions In order to study fluid behaviors under influencing factors of cryogenic capillary-flow under microgravity, a 2d numerical model of vertical capillary tube is constructed in the paper showed in the Fig.1 and physical properties of working fluids are shown in Table 1. In order to save computational resources, a 2D axisymmetric numerical model is adopted in the paper. The model radius of capillary tube is 0.2 mm, 1mm respectively, along with the height of the model is 50 mm. Initially, the capillary channel is filled with most of the gas (upper) and a small amount of liquid (lower), and the capillary tension causes the liquid to rise. The initial height of liquid is 1 mm, 10 mm respectively in this paper. The static contact angle of the wetted wall in the model which is the angle between the surface of the water and the wall surface, is chosen to be 68°. The upper and lower boundary of the model are respectively the pressure outlet and pressure inlet boundary conditions.

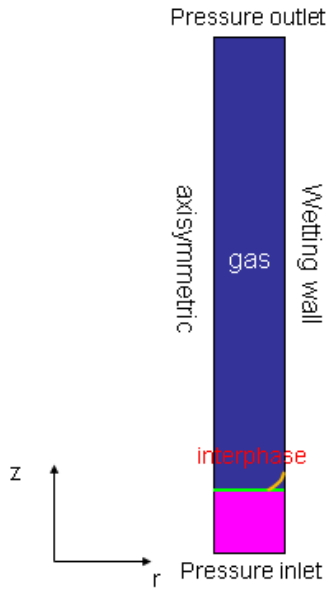

Figure 1. Geometry model and boundary conditions for numerical simulation

Table 1
Physical properties of working fluids

Working fluid	Working temperature (℃)	Density (kg/m^3)	Kinetic viscosity (Pa*s)	Surface tension (N/m)
Water	20	1000	$1.003e^{-3}$	0.0727
Air		1.225	$1.789e^{-5}$	
Ne (liquid)	-249	1223.4868	$1.281e^{-4}$	$5.114e^{-3}$
Ne (gas)		7.2985	$4.366e^{-6}$	
N_2 (liquid)	-200	824.8498	$1.912e^{-4}$	$9.842e^{-3}$

N_2 (gas)		2.8403	$5.121e^{-6}$	
He (liquid)	-269.5	134.1618	$3.446e^{-6}$	$1.470e^{-4}$
He (gas)		9.4746	$1.018e^{-6}$	

Calculation of Working Conditions In this paper, there are four working cases which would be calculated and analyzed in the following:

- **Case 1:** The comparisons among various low-temperature working fluids (Ne, He and N_2) for the capillary tube radius r=0.2mm under microgravity.
- **Case 2:** The comparisons among various capillary tube radii (r=0.2mm, 0.6mm and 1mm) for Ne working fluid under microgravity.
- **Case 3:** The comparisons among various initial liquid volumes (initial interface height is 1mm, 10mm, respectively) for the capillary tube radius r=0.2mm and Ne working fluid.under microgravity.
- **Case 4:** The comparisons among various initial liquid volumes (initial interface height is 1mm, 10mm, respectively) for the capillary tube radius r=1mm and Ne working fluid.under microgravity.

NUMERICAL MODEL VALIDATION

In order to verify the accuracy and rationality of this numerical method, the first thing needs to do is to test the capillary height of interphase in the gravity field. Water and air at room temperature are chose as the testing liquid and gas, and their physical properties are shown in Table 1. The verification model, boundary conditions, and initial conditions are shown in Fig.1. The model radius of capillary tube is 0.2 mm and the height is 35 mm in this 2D verification model, along with the height of the initial interface is 1 mm and the static contact angle is 68°. The acceleration of gravity here is 9.8 m/s^2.

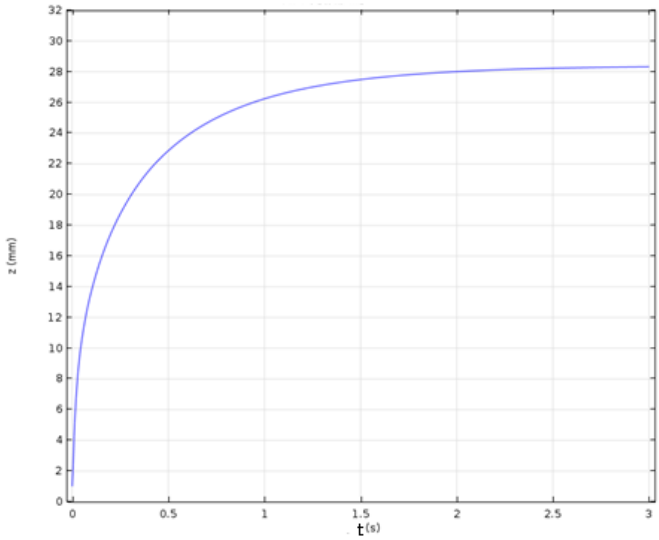

Figure 2. The change trend of the height Z of interphase dynamic contact point with time t under gravity

From Fig.2, it can be seen that the height Z of the interphase dynamic contact point on the wetting wall increases with the time t under gravity. The contact point height Z approaches to 28.2 mm at t= 0.4s under gravity. The relative error between the numerical model and the theoretical formula $\rho gh = \frac{2\sigma}{R} = 27.8mm$ is 1.44% under gravity, which proves the accuracy and rationality of the numerical method here.

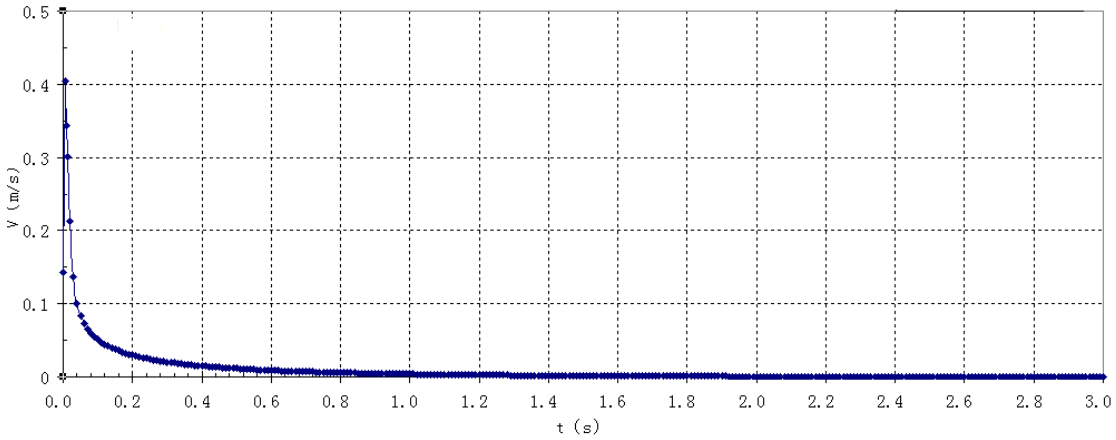

Figure 3. The change trend of the velocity of interphase dynamic contact point with time t under gravity

From Fig.3, it can be seen that the velocity of interphase dynamic contact point on the wetting wall under gravity reaches the maximum 0.41 m/s at t = 0.01s, while it is increasing sharply at t <0.01s and decreases rapidly at t> 0.01s. After time t = 0.4s, the velocity of interphase dynamic contact point on the wetting wall is almost close to zero under gravity.

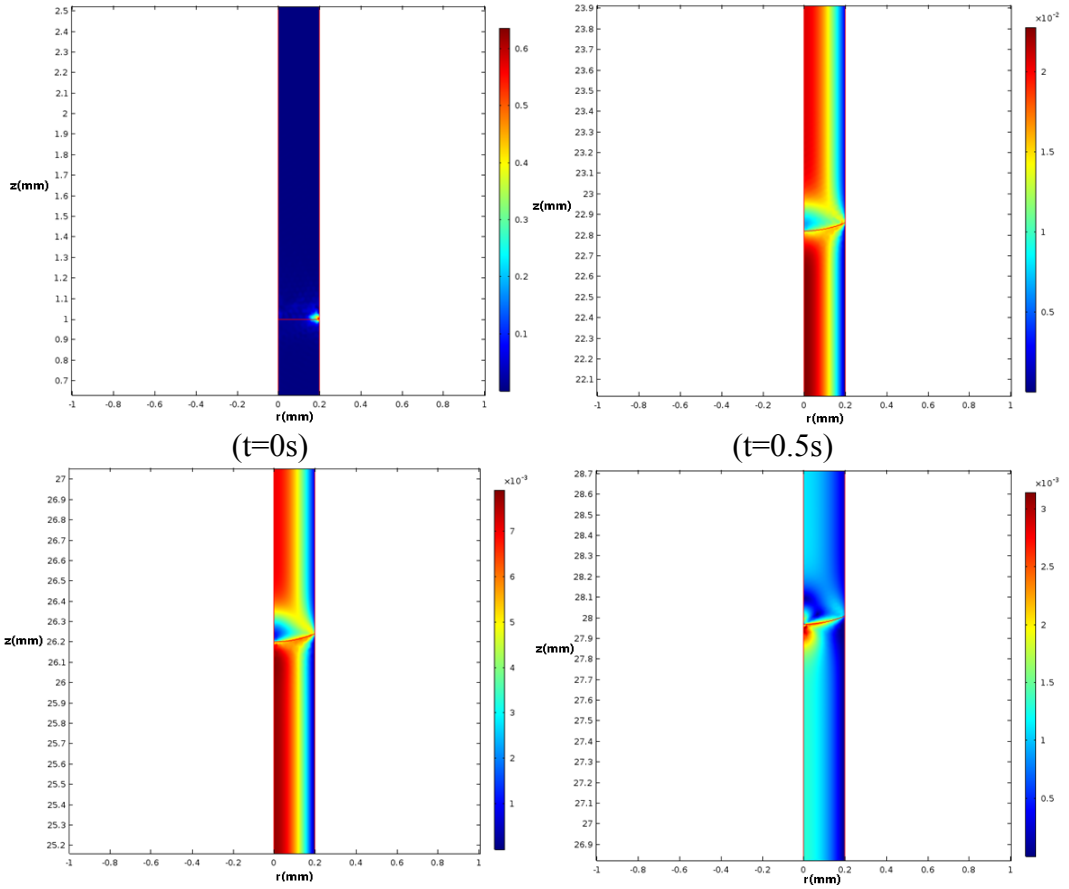

(t=0s) (t=0.5s)

(t=1s) (t=2s)

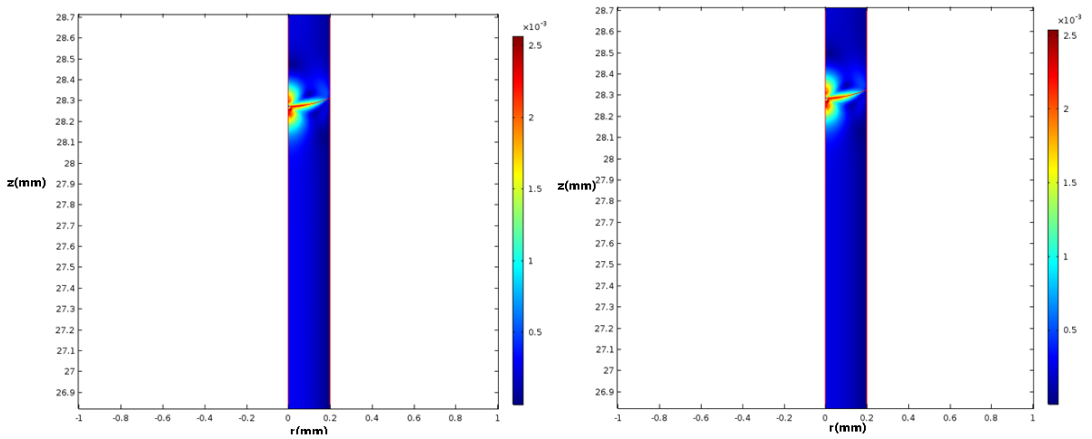

(t=2.9s) (t=3s)

Figure 4. The velocity contour of the whole flow field under gravity

It can be seen that the velocity of the whole flow field (water and air) decreases rapidly as time under gravity in Fig.4.

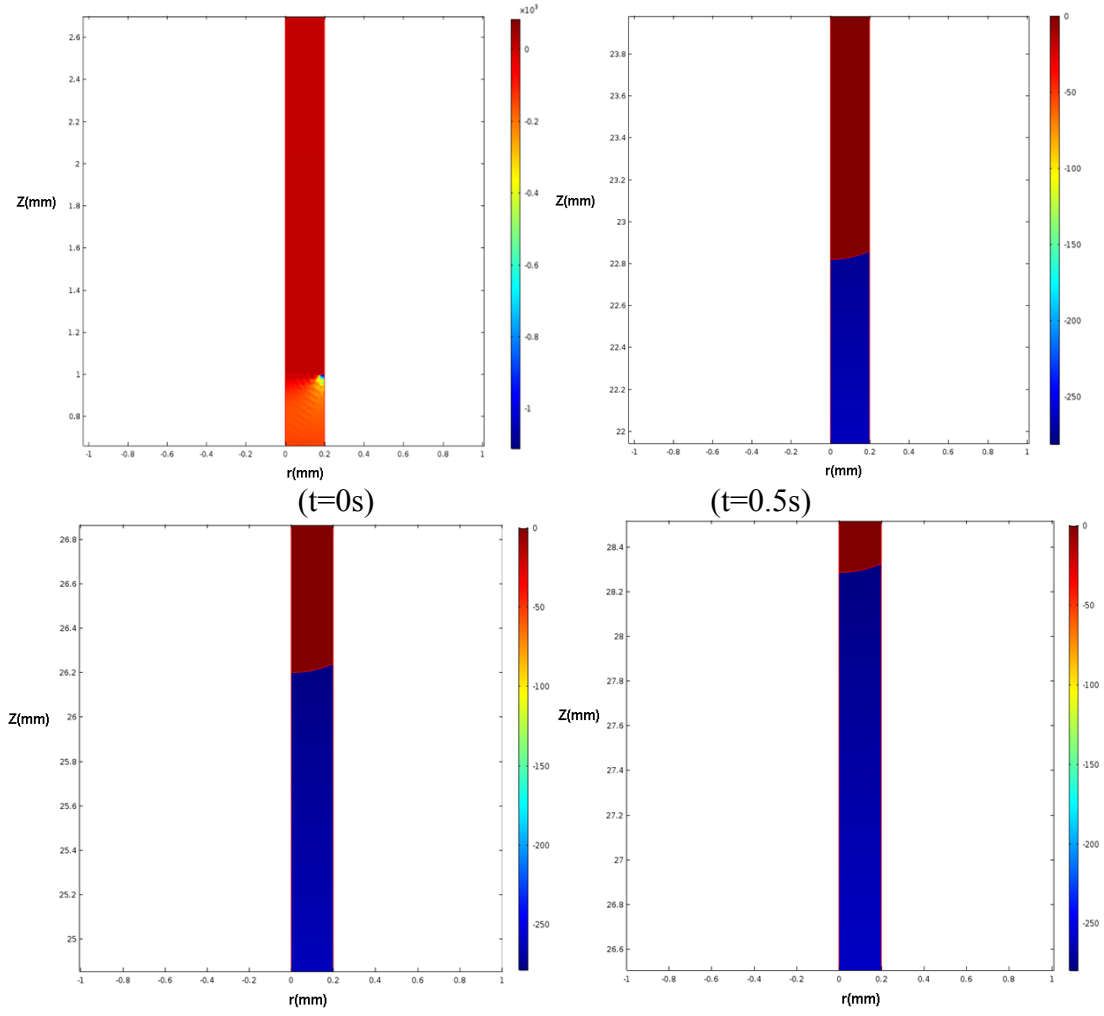

(t=0s) (t=0.5s)

(t=1s) (t=3s)

Fig.5 The pressure contour part magnification around the interface of the whole flow field under gravity

RESULTS AND DISCUSSION

Case 1 The change trend comparisons of height and velocity of interphase dynamic contact point on the wetting wall with time t among various low-temperature working fluids (Ne, He and N_2) are shown in Fig.6 and Fig.7 separately, which are in the model of capillary tube diameter r=0.2 mm under microgravity.

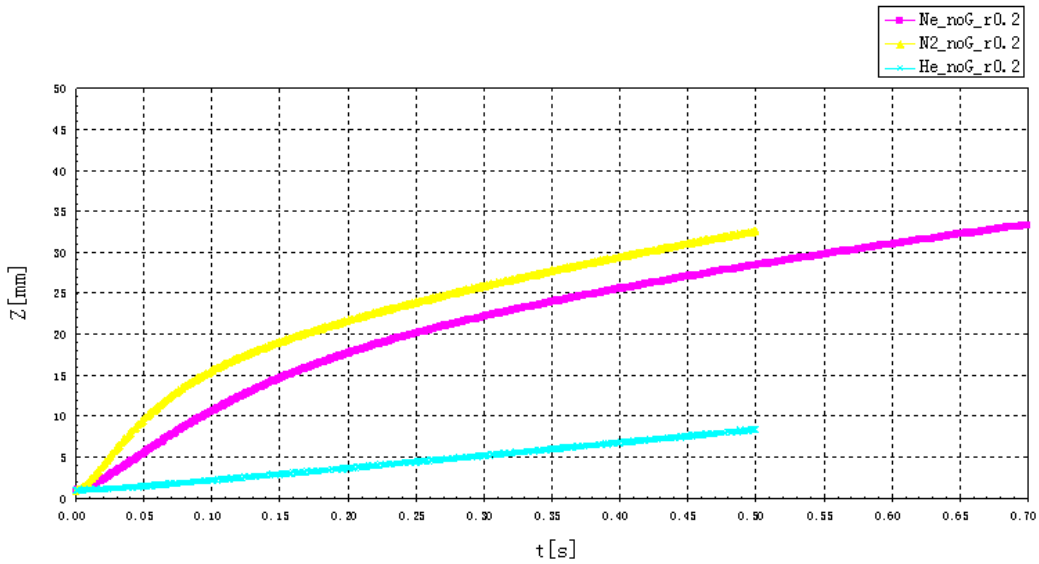

Figure 6. The height change trend of interphase dynamic contact point for low-temperature working fluids under microgravity

From Fig.6, it can be seen that the height Z of the interphase dynamic contact point on the wetting wall increases with the time t under microgravity for various low-temperature working fluids (Ne, He and N_2). Among them, the height increasing trend with time for N_2 is the largest, followed by Ne, and finally He.

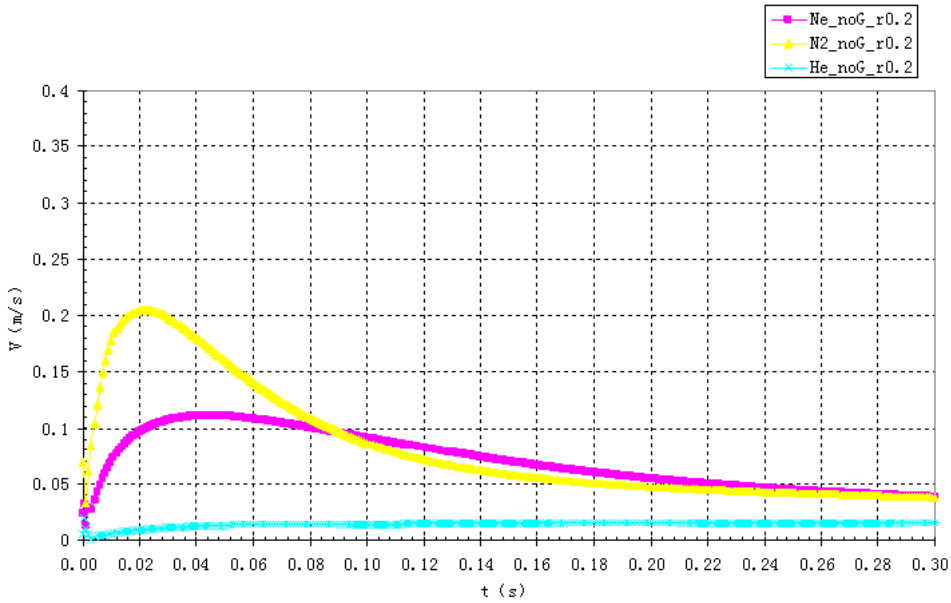

Figure 7. The velocity change trend of interphase dynamic contact point for low-temperature working fluids under microgravity

From Fig.7, it can be seen that the velocity V of the interphase dynamic contact point on the wetting wall increases sharply at first with the time t and then decrease rapidly to the same value 0.04 m/s under microgravity for low-temperature working fluids N_2 and Ne, which reaches the maximum 0.2 m/s at t =

0.01s, 0.12 m/s at t=0.04, respectively. For He, the velocity trend of the interphase dynamic contact point on the wetting wall increases gradually to 0.02 m/s with the time t under microgravity.

Therefore, it shows an upward trend for the height of the interphase dynamic contact point on the wetting wall toward various low-temperature working fluids (Ne, He and N_2) for the capillary tube diameter r=0.2 mm under microgravity, but the corresponding velocity trend has a great relationship with the low-temperature working fluid.

Case 2 The change trend comparisons of height and velocity of interphase dynamic contact point on the wetting wall with time t among various capillary tube radii (r=0.2 mm, 0.6 mm and 1 mm) are shown in Fig.8 and Fig.9 separately, which are for Ne working fluid under microgravity.

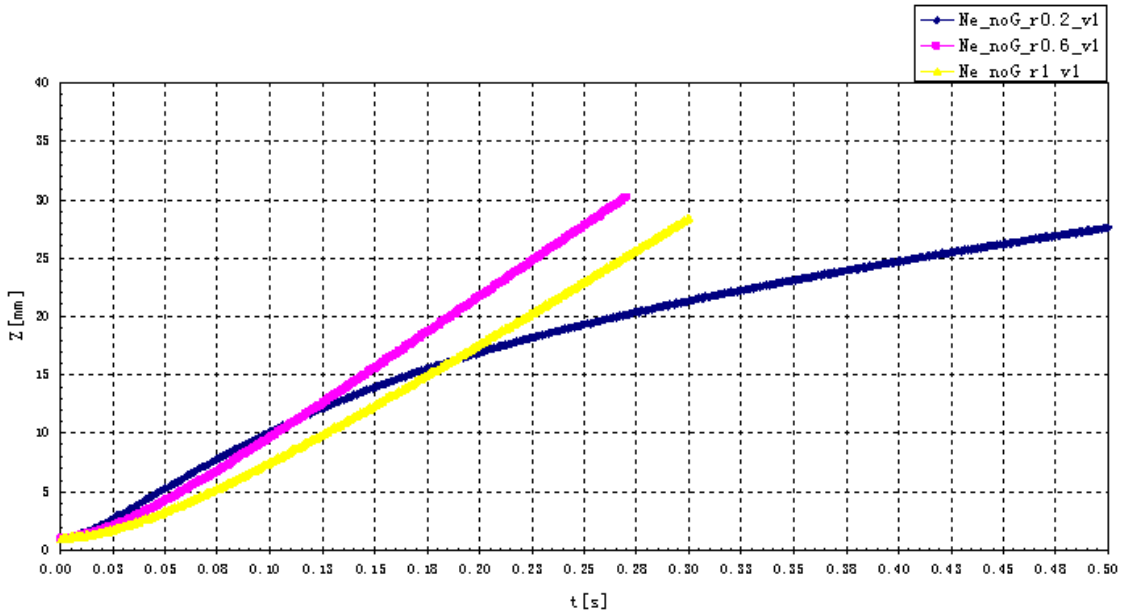

Figure 8. The height change trend of interphase dynamic contact point among various capillary tube radii for Ne under microgravity

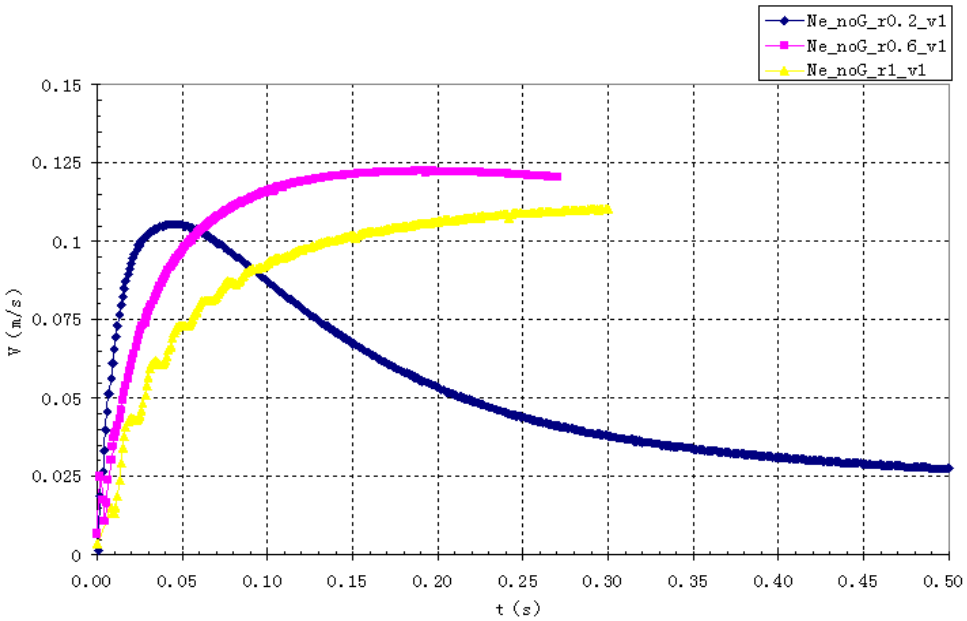

Figure 9. The velocity change trend of interphase dynamic contact point among various capillary tube radii for Ne under microgravity

From Fig.9, we can see that before t=0.04 s, the velocity of the interphase dynamic contact point on the wetting wall for r=0.2 mm under microgravity is larger than that of r=0.6 mm, and the corresponding velocity for r=0.6 mm is also larger than that of r=1mm under microgravity. But after t=0.04s, the corresponding velocity began to decrease for r=0.2 mm, while it increases slowly after t=0.125s and t=0.19s, respectively for r=0.6 mm and 1mm under microgravity. So it can be seen that the height of the interphase dynamic contact point on the wetting wall for r=0.6 mm tends to exceed that of r=0.2 mm after t=0.125s under microgravity, while the corresponding velocity of r=1 mm larger tends to exceed that of r=0.2 mm after t=0.19s under microgravity showed in Fig.8.

Therefore, it shows an upward trend for the height of the interphase dynamic contact point on the wetting wall toward various capillary tube radii (r=0.2 mm, 0.6mm and 1mm) for Ne working fluid under microgravity, but the corresponding velocity trend has a great relationship with the capillary tube radius.

Case 3 The change trend comparisons of height and velocity of interphase dynamic contact point on the wetting wall with time t for various initial liquid volumes (initial interface height 1 mm and10 mm) are shown in Fig.10 and Fig.11 separately, which are for the capillary tube radius r = 0.2 mm and Ne working fluid under microgravity.

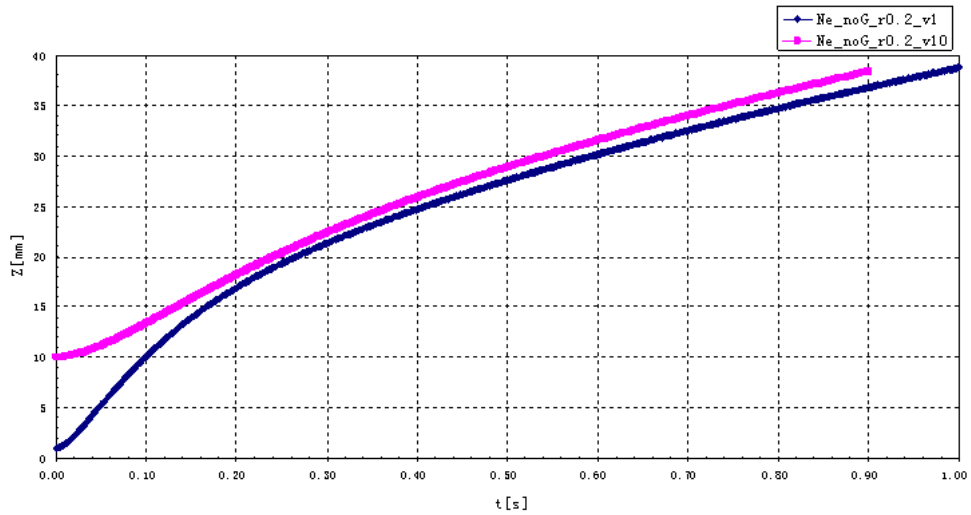

Figure 10. The height change trend of interphase dynamic contact point among various initial liquid volumes for Ne and capillary tube radius r=0.2mm under microgravity

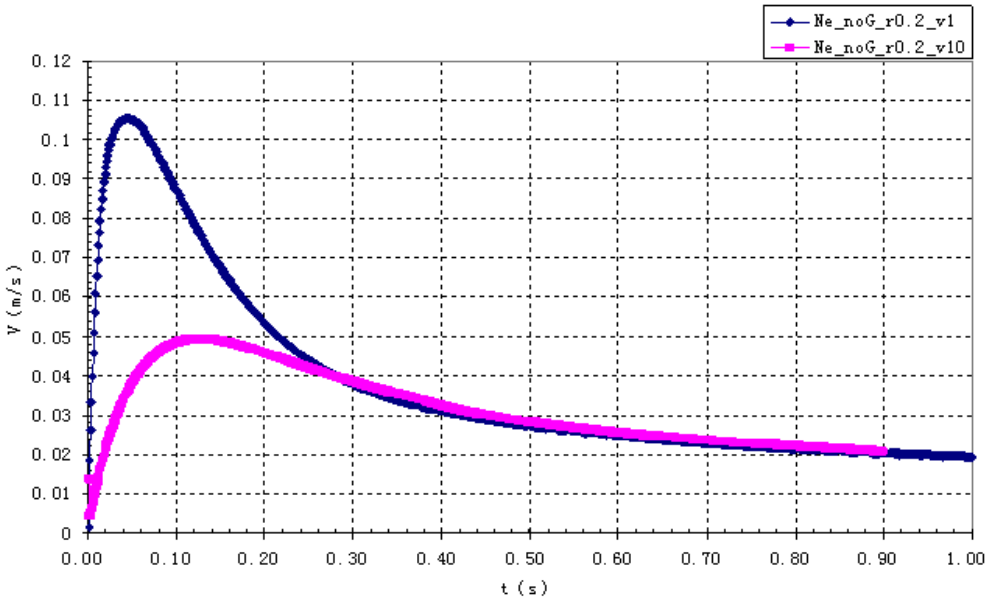

Figure 11. The velocity change trend of interphase dynamic contact point among various initial liquid volumes for Ne and capillary tube radius r=0.2mm under microgravity

As Fig.10 shows that the velocity of the interphase dynamic contact point on the wetting wall for the initial interface height 1mm is much larger than that of the initial interface height 10mm before t=0.28s, and the corresponding maximal velocity of the interphase dynamic contact point for the initial interface height 1mm reaches 0.105m/s. After t=0.28s, the corresponding velocity of the interphase dynamic contact point is almost the same for various initial liquid volumes. So the corresponding height of the interphase dynamic contact point on the wetting wall maintains a parallel upward trend for various initial liquid volumes after t=0.28s showed in Fig.9.

Case 4 The change trend comparisons of height and velocity of interphase dynamic contact point on the wetting wall with time t for various initial liquid volumes (initial interface height 1 mm and10 mm) are shown in Fig.12 and Fig.13 separately, which are for the capillary tube radius r=1mm and the Ne working fluid under microgravity.

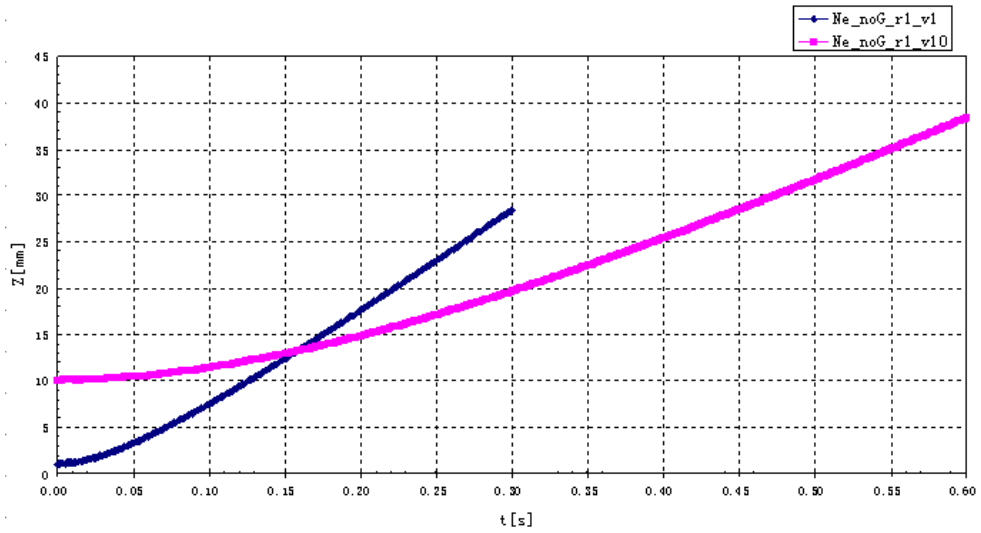

Figure 12. The height change trend of interphase dynamic contact point among various initial liquid volumes for Ne and capillary tube radius r=1mm under microgravity

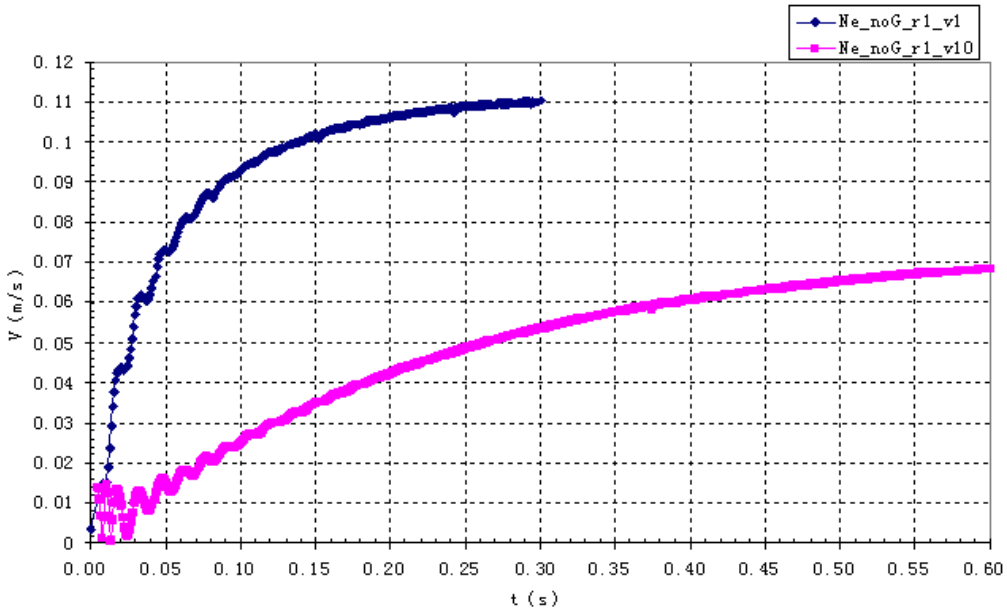

Figure 13. The velocity change trend of interphase dynamic contact point among various initial liquid volumes for Ne and capillary tube radius r=1mm under microgravity

It can be seen from Fig.13 that the velocity of the interphase dynamic contact point on the wetting wall increases steadily with the time t under microgravity, which finally approximates to 0.11m/s for the initial interface height 1mm and 0.06m/s for the initial interface height 10mm, respectively. So it shows that the height of the interphase dynamic contact point on the wetting wall for the initial interface height 1mm increases sharply and then exceed the corresponding height for the initial interface height 10 mm after t=0.15s under microgravity showed in Fig.12.

CONCLUSIONS

As we all known, the surface tension of cryogenic fluids in deep low-temperature space is much smaller, so the capillary driven by surface tension is weakened under microgravity, which is influenced by many factors, including the working fluid properties, the wettability of capillary surface, and the geometrical properties of tube (cross-sectional shape, equivalent diameter, wetted perimeter, etc.). In the paper, fluid behaviors under influencing factors (including tube sizes, low-temperature working fluid properties, initial liquid volumes, etc.) of cryogenic capillary-flow under microgravity are studied numerically by developing a 2D numerical simulation of vertical capillary tube based on the moving mesh interface method, which represent the interface between two phases by a no thickness boundary. To verify accuracy and rationality of this numerical method, the capillary height of interphase between water and air at room temperature in the gravity field is tested firstly, in which the relative results prove that the accuracy and rationality of this numerical method here. Then, the numerical simulation is carried out for four working cases.

From the results in Case 1, we can see that there is an upward trend for the height of the interphase dynamic contact point on the wetting wall toward various low-temperature working fluids (Ne, He and N2) for the capillary tube diameter r=0.2mm under microgravity, but the corresponding velocity trend has a great relationship with the low-temperature working fluid. It is clear that N2 is the best cryogenic fluid here, which is more suitable in deep low-temperature space. It also shows an upward trend in Case 2 for the height of the interphase dynamic contact point toward various capillary tube radii (r=0.2mm, 0.6mm and 1mm) for Ne under microgravity, but the corresponding velocity trend has a great relationship with the capillary tube radius.

Although there are some small differences which are brought by the different velocity trend of the interphase dynamic contact point in Case 3 and 4, it shows an increasing trend on the whole in the height of the interphase dynamic contact point on the wetting wall for various initial interface heights for Ne under microgravity, either the capillary tube radius r=0.2mm or r=1mm.

STATEMENT ON NUMERICAL ACCURACY

The numerical modelling made in this work was strictly followed the statement of the simulation conditions. Accuracy of the results were ensured by the following criteria as we stated in the text.

REFERENCES

Lucas, R. [1918], Üeber das Zeitgesetz des Kapillaren Aufstiegs von Flüssigkeiten, *Kolloid Zeitschrift and Zeitschrift für Polymere*, Vol. 23, No. 1, pp 15-22.

Washburn, E. W. [1921], The Dynamics of Capillary Flow, *Physical Review*, Vol. 17, No. 3, pp 273-283.

Bell, J. M., and Cameron, F. K. [1906], The Flow of Liquids Through Capillary Spaces, *Journal of Physical Chemistry*, Vol. 10, No. 8, pp 658-674.

Dreyer, M. E., Gerstmann, J., Stange, M., Rosendahl, U., Wölk, G., and Rath, H. J. [1998], Capillary Effects Under Low Gravity, Part 1: Surface Settling, Capillary Rise, and Critical Velocities, *Space Forum*, Vol. 3, pp 87-136.

Dreyer, M. E., Delgado, A, and Rath, H. J. [1994], Capillary Rise of Liquid Between Parallel Plates Under Microgravity, *Journal of Colloid and Interface Science*, Vol. 163, No. 1, pp 158-168.
Weislogel, M. M., and Lichter, S. [1998], Capillary Flow in an Interior Corner, *Journal of Fluid Mechanics*, Vol. 373, No. 1, pp 349-378.
Chen, Y., and Collicott, S. [2005], Experimental Study on Capillary Flow in a Vane-Wall Gap Geometry, *AIAA Journal*, Vol. 43, No. 11, pp 2395-2403.
Concus, P., Finn, R., and Weislogel, M. [2000], Measurement of Critical Contact Angle in a Microgravity Space Experiment, *Experiments in Fluids*, Vol. 28, No. 3, pp 197-205.
Stange, M., Dreyer, M. E., and Rath, H. J. [2003], Capillary-Driven Flow in Circular Cylindrical Tubes, *Physics of Fluids*, Vol. 15, No. 9, pp 2587-2601.
Wang, C., Xu, S., Sun, Z. and Hu, W. [2009], Influence of Contact Angle and Tube Size on Capillary-Driven Flow Under Microgravity, *AIAA Journal*, Vol. 47, No. 11, pp 2642-2648.